

ESTIMATING THE TWO-DIMENSIONAL COHERENCE FUNCTION

Andreas Jakobsson*, Stephen R. Alty† and Jacob Benesty‡

*Department of Electrical Engineering, Karlstad University, Sweden

†King's College London, Centre for Digital Signal Processing Research, UK

‡Université du Québec, INRS-EMT, Canada

ABSTRACT

In this paper, we extend the one-dimensional Capon-based Magnitude Square Coherence (MSC) spectral estimator, to form two-dimensional Capon- and APES-based MSC spectral estimators. The resulting estimators are found to yield significantly improved estimates as compared to the typical Welch-based estimator. Furthermore, we introduce a computationally efficient time-updating of the presented MSC estimators, exploiting their inherent time-varying displacement structure. The presented updating is found to dramatically lower the computational requirement of reevaluating the MSC spectral estimates.

Index Terms— Coherence estimation, spectral analysis, multidimensional signal processing, displacement structure

1. INTRODUCTION

Spectral estimation finds applications in a wide range of fields, and has received a vast amount of interest in the literature over the last century. Due to their inherent robustness to model assumptions, there has lately been a renewed interest in non-parametric spectral estimators. Among the non-parametric approaches, the data-dependent filterbank spectral estimators have many desirable properties. In particular, there has been a substantial interest in the Capon and the APES spectral estimators [1], which have been shown to offer very accurate, computationally efficient, high-resolution estimates (see, e.g., [2] and the many references therein). In this paper, we consider the estimation of the Magnitude Square Coherence (MSC) spectrum between two images. Even though the MSC spectrum is useful in a wide variety of applications, such as for instance SAR imagery (see, e.g., [3, 4]), few methods exist for forming an accurate high-resolution estimate of the spectrum. Recently, a one-dimensional (1-D) Capon-based MSC estimator was introduced in [5]. As was shown in [5], the Capon-based estimate offered a significantly improved resolution as compared to the popular Welch's method. Herein, we extend this estimator to form both a 2-D Capon-based and a 2-D APES-based MSC estimator. Furthermore, exploiting

the time-varying displacement (TVD) structure of the presented estimators, we derive efficient forward-backward averaged (FBA), sliding window, time-updating algorithms for these estimators (we refer the reader to [6] for a further discussion on displacement theory).

2. ESTIMATING THE MSC SPECTRUM

We define the 2-D MSC spectrum between two $N \times \bar{N}$ data images $x_1(n, \bar{n})$ and $x_2(n, \bar{n})$ as (see, e.g., [3])

$$\gamma_{\omega, \bar{\omega}} = \frac{|\phi_{x_1 x_2}(\omega, \bar{\omega})|^2}{\phi_{x_1 x_1}(\omega, \bar{\omega}) \phi_{x_2 x_2}(\omega, \bar{\omega})}, \quad (1)$$

where $\phi_{x_k x_p}(\omega, \bar{\omega})$ denotes the 2-D cross-spectrum between $x_k(n, \bar{n})$ and $x_p(n, \bar{n})$, defined as

$$\phi_{x_k x_p}(\omega, \bar{\omega}) = \sum_{l, \bar{l}=-\infty}^{\infty} r_{x_k x_p}(l, \bar{l}) e^{-i(\omega l + \bar{\omega} \bar{l})}, \quad (2)$$

for $k, p = 1, 2$, with $r_{x_k x_p}(l, \bar{l}) = E\{x_k(n, \bar{n})x_p^*(n-l, \bar{n}-\bar{l})\}$, and $E\{\cdot\}$ and $(\cdot)^*$ denoting the expectation and the Hermitian, respectively. Forming the $MM \times 1$ vectorized submatrices $\mathbf{y}_{l, \bar{l}}^k = \text{vec}\{\mathbf{Y}_{l, \bar{l}}^k\}$ with $\text{vec}\{\mathbf{X}\}$ denoting the operation stacking the columns of the matrix \mathbf{X} on top of each other, from the data available at time t , where

$$\mathbf{Y}_{l, \bar{l}}^k = \begin{bmatrix} x_k(l, \bar{l} - \bar{M} + 1) & \dots & x_k(l, \bar{l}) \\ \vdots & \ddots & \vdots \\ x_k(l + M - 1, \bar{l} - \bar{M} + 1) & \dots & x_k(l + M - 1, \bar{l}) \end{bmatrix}$$

for $l = 0, \dots, L-1, \bar{l} = 0, \dots, \bar{L}-1$, where $L = N - M + 1$ and $\bar{L} = \bar{N} - \bar{M} + 1$, the 2-D Capon and APES filters¹ may be formed as (see, e.g., [2])

$$\mathbf{h}_{\omega, \bar{\omega}}^C = \frac{\mathbf{R}_{x_k x_k}^{-1} \mathbf{a}_{\omega, \bar{\omega}}}{\mathbf{a}_{\omega, \bar{\omega}}^* \mathbf{R}_{x_k x_k}^{-1} \mathbf{a}_{\omega, \bar{\omega}}}, \quad (3)$$

$$\mathbf{h}_{\omega, \bar{\omega}}^A = \frac{\mathbf{Q}_{x_k x_k}^{-1} \mathbf{a}_{\omega, \bar{\omega}}}{\mathbf{a}_{\omega, \bar{\omega}}^* \mathbf{Q}_{x_k x_k}^{-1} \mathbf{a}_{\omega, \bar{\omega}}}, \quad (4)$$

¹We note that the form of the FBA APES filter will differ from the forward-only APES filter. Herein, we consider the FBA version, formed using the noise covariance matrix estimate in (7).

Please address all correspondence to Andreas Jakobsson (andreas.jakobsson@ieee.org).

where $\mathbf{a}_{\omega, \bar{\omega}} = \mathbf{a}_{\omega} \otimes \bar{\mathbf{a}}_{\bar{\omega}}$, with \otimes denoting the Kronecker product,

$$\mathbf{a}_{\omega} = [1 \quad e^{i\omega} \quad \dots \quad e^{i\omega(M-1)}]^T, \quad (5)$$

$$\bar{\mathbf{a}}_{\bar{\omega}} = [1 \quad e^{i\bar{\omega}} \quad \dots \quad e^{i\bar{\omega}(\bar{M}-1)}]^T, \quad (6)$$

and $\mathbf{R}_{x_k x_p}$ is the (scaled) covariance matrix of $\mathbf{y}_{l, \bar{l}}^k$, discussed further below. Furthermore, $\mathbf{Q}_{x_k x_k}$ is formed as an estimate of the covariance matrix of all signal components at frequencies different from $(\omega, \bar{\omega})$, i.e., [1]

$$\begin{aligned} \mathbf{Q}_{x_k x_k} &= \mathbf{R}_{x_k x_k} - \frac{1}{2L\bar{L}} [\mathbf{g}_k \quad \check{\mathbf{g}}_k] \begin{bmatrix} \mathbf{g}_k^* \\ \check{\mathbf{g}}_k^* \end{bmatrix}, \\ &\triangleq \mathbf{R}_{x_k x_k} - \mathbf{G}_k \mathbf{G}_k^* \end{aligned} \quad (7)$$

where

$$\mathbf{g}_k = \sum_{l=0}^{L-1} \sum_{\bar{l}=0}^{\bar{L}-1} \mathbf{y}_{l, \bar{l}}^k e^{-i\omega l - i\bar{\omega}(\bar{L}-1-\bar{l})}, \quad (8)$$

$$\check{\mathbf{g}}_k = \sum_{l=0}^{L-1} \sum_{\bar{l}=0}^{\bar{L}-1} \check{\mathbf{y}}_{l, \bar{l}}^k e^{-i\omega l - i\bar{\omega}(\bar{L}-1-\bar{l})}, \quad (9)$$

with $\check{\mathbf{y}}_{l, \bar{l}}^k$ denoting the (l, \bar{l}) th backward data vector formed similar to $\mathbf{y}_{l, \bar{l}}^k$, but from the backward data matrix (see, e.g., [1,2] for further details). It is worth noting that $\mathbf{Q}_{x_k x_k}$ will depend on $(\omega, \bar{\omega})$. We proceed to form the corresponding spectral estimates as the power of the filter output², i.e.,

$$\phi_{x_k x_p}(\omega, \bar{\omega}) = \frac{\mathbf{h}_{x_k}^* \mathbf{R}_{x_k x_p} \mathbf{h}_{x_p}}{L\bar{L}}, \quad (10)$$

where \mathbf{h}_{x_k} denotes either of the filters in (3) or (4) formed on the image $x_k(n, \bar{n})$, implying that the Capon- and APES-based MSC estimates, formed from (1), can be expressed as

$$\gamma_{\omega, \bar{\omega}}^C = \frac{\left| \mathbf{a}_{\omega, \bar{\omega}}^* \mathbf{R}_{x_1 x_1}^{-1} \mathbf{R}_{x_1 x_2} \mathbf{R}_{x_2 x_2}^{-1} \mathbf{a}_{\omega, \bar{\omega}} \right|^2}{\left(\mathbf{a}_{\omega, \bar{\omega}}^* \mathbf{R}_{x_1 x_1}^{-1} \mathbf{a}_{\omega, \bar{\omega}} \right) \left(\mathbf{a}_{\omega, \bar{\omega}}^* \mathbf{R}_{x_2 x_2}^{-1} \mathbf{a}_{\omega, \bar{\omega}} \right)} \quad (11)$$

$$\gamma_{\omega, \bar{\omega}}^A = \frac{\left| \mathbf{a}_{\omega, \bar{\omega}}^* \mathbf{Q}_{x_1 x_1}^{-1} \mathbf{R}_{x_1 x_2} \mathbf{Q}_{x_2 x_2}^{-1} \mathbf{a}_{\omega, \bar{\omega}} \right|^2}{\prod_{k=1}^2 \mathbf{a}_{\omega, \bar{\omega}}^* \mathbf{Q}_{x_k x_k}^{-1} \mathbf{R}_{x_k x_k} \mathbf{Q}_{x_k x_k}^{-1} \mathbf{a}_{\omega, \bar{\omega}}} \quad (12)$$

Introducing

$$\boldsymbol{\mu}_k = \mathbf{L}_{x_k} \mathbf{a}_{\omega, \bar{\omega}}, \quad (13)$$

where \mathbf{L}_{x_k} denotes the (unique) lower-triangular Cholesky factor of $\mathbf{R}_{x_k x_k}^{-1}$, such that $\mathbf{R}_{x_k x_k}^{-1} = \mathbf{L}_{x_k}^* \mathbf{L}_{x_k}$, the Capon-based MSC estimator in (11) can be expressed as

$$\gamma_{\omega, \bar{\omega}}^C = \frac{\left| \boldsymbol{\mu}_1^* \mathbf{L}_{x_1} \mathbf{R}_{x_1 x_2} \mathbf{L}_{x_2}^* \boldsymbol{\mu}_2 \right|^2}{\left| \boldsymbol{\mu}_1 \right|^2 \left| \boldsymbol{\mu}_2 \right|^2}. \quad (14)$$

²We remark that the APES technique is commonly used to form the amplitude and phase spectral estimate. Herein, we prefer to form the APES power spectral estimate. In general, these two estimates will differ.

Similarly, using the matrix inversion lemma to expand (7), as well as exploiting that $\mathbf{L}_{x_k} \mathbf{R}_{x_k x_k} \mathbf{L}_{x_k}^* = \mathbf{I}_{M\bar{M}}$, (12) can be expressed as

$$\gamma_{\omega, \bar{\omega}}^A = \frac{\left| \check{\boldsymbol{\mu}}_1^* \mathbf{L}_{x_1} \mathbf{R}_{x_1 x_2} \mathbf{L}_{x_2}^* \check{\boldsymbol{\mu}}_2 \right|^2}{\left| \check{\boldsymbol{\mu}}_1 \right|^2 \left| \check{\boldsymbol{\mu}}_2 \right|^2}, \quad (15)$$

where $\check{\boldsymbol{\mu}}_k = \check{\boldsymbol{\Phi}}_k \boldsymbol{\mu}_k$, $\check{\boldsymbol{\Phi}}_k = \mathbf{I}_{M\bar{M}} + \boldsymbol{\nu}_k^* [\mathbf{I}_2 - \boldsymbol{\nu}_k \boldsymbol{\nu}_k^*]^{-1} \boldsymbol{\nu}_k$, and

$$\boldsymbol{\nu}_k = \mathbf{G}_k^* \mathbf{L}_{x_k}^*, \quad (16)$$

with \mathbf{I}_P denoting the $P \times P$ identity matrix. Paralleling [5], we note that both (14) and (15) will be limited to $0 \leq \gamma_{\omega, \bar{\omega}} \leq 1$. Further, from both (14) and (15), we note that the main complexity in forming the estimates, for each frequency grid point $(\omega, \bar{\omega})$, will be in evaluating \mathbf{L}_{x_k} . We also remark that, given the rich structure of these estimators, both will allow for efficient implementations using techniques similar to the ones presented in [7] and [8]. Finally, we note that $\mathbf{R}_{x_k x_k}$ and $\mathbf{R}_{x_k x_p}$ are typically unknown, and should therefore be replaced by consistent estimates; herein, we use the FBA covariance matrix estimate to form $\hat{\mathbf{R}}_{x_k x_k}$, as it is known to yield preferable spectral estimates, i.e.,

$$\hat{\mathbf{R}}_{x_k x_k} = \frac{1}{2} \left(\hat{\mathbf{R}}_{x_k x_k}^f + \mathbf{J} \hat{\mathbf{R}}_{x_k x_k}^{fT} \mathbf{J} \right), \quad (17)$$

where \mathbf{J} denotes the exchange matrix, and

$$\hat{\mathbf{R}}_{x_k x_k}^f = \sum_{l=0}^{L-1} \sum_{\bar{l}=0}^{\bar{L}-1} \mathbf{y}_{l, \bar{l}}^k \mathbf{y}_{l, \bar{l}}^{k*}. \quad (18)$$

Similarly, $\hat{\mathbf{R}}_{x_k x_p}$ is formed using the forward-only estimate. In the following section, we will proceed to examine how to update the 2-D MSC estimates as additional data becomes available.

3. TIME-UPDATING THE MSC ESTIMATES

Given the centrohermitian structure of $\mathbf{R}_{x_k x_k}$, one may form the decomposition [9], $\mathbf{R}_{x_k x_k} = \mathbf{K} \mathbf{B}_{x_k x_k} \mathbf{K}^*$, where \mathbf{K} can be selected to be column conjugate symmetric³ and unitary. In particular, for even dimension $\mathbf{R}_{x_k x_k}$,

$$\mathbf{K} = \frac{1}{\sqrt{2}} \begin{bmatrix} \mathbf{I} & i\mathbf{I} \\ \mathbf{J} & -i\mathbf{J} \end{bmatrix}, \quad (19)$$

where \mathbf{K} is a square matrix with the same dimensions as $\mathbf{R}_{x_k x_k}$. Similarly, for odd dimension $\mathbf{R}_{x_k x_k}$,

$$\mathbf{K} = \frac{1}{\sqrt{2}} \begin{bmatrix} \mathbf{I} & 0 & i\mathbf{I} \\ 0 & i\sqrt{2} & 0 \\ \mathbf{J} & 0 & -i\mathbf{J} \end{bmatrix}. \quad (20)$$

³A matrix \mathbf{K} is said to be column conjugate symmetric if $\mathbf{K} = \mathbf{J} \mathbf{K}^*$.

For this choice of \mathbf{K} , $\mathbf{B}_{x_k x_k}$ is a real symmetric matrix. As shown in [9], this decomposition offers a significant complexity reduction for the most common operations on FBA covariance matrices, such as the time-updating of $\mathbf{R}_{x_k x_k}$. Let the FBA covariance matrix estimate at time t be denoted $\mathbf{R}_{x_k x_k}^t$. Then, the time-update, such that

$$\hat{\mathbf{R}}_{x_k x_k}^t = \hat{\mathbf{R}}_{x_k x_k}^{t-1} + \hat{\mathbf{Y}}_t^k \hat{\mathbf{Y}}_t^{k*} - \check{\mathbf{Y}}_t^k \check{\mathbf{Y}}_t^{k*}, \quad (21)$$

where

$$\hat{\mathbf{Y}}_t^k = \begin{bmatrix} \mathbf{Y}_t^{k,f} & \mathbf{J}\mathbf{Y}_t^{k,f} \end{bmatrix} \quad (22)$$

$$\check{\mathbf{Y}}_t^k = \begin{bmatrix} \mathbf{Y}_{t-\bar{N}}^{k,f} & \mathbf{J}\mathbf{Y}_{t-\bar{N}}^{k,f} \end{bmatrix} \quad (23)$$

denote the updating and the downdating data matrices, respectively, with

$$\mathbf{Y}_t^{k,f} = \begin{bmatrix} \mathbf{y}_{0,t}^k & \cdots & \mathbf{y}_{L-1,t}^k \end{bmatrix}, \quad (24)$$

$$\mathbf{Y}_{t-\bar{N}}^{k,f} = \begin{bmatrix} \mathbf{y}_{0,t-\bar{N}}^k & \cdots & \mathbf{y}_{L-1,t-\bar{N}}^k \end{bmatrix}, \quad (25)$$

can preferably⁴ be formed as $\hat{\mathbf{R}}_{x_k x_k}^t = \mathbf{K}\mathbf{B}_{x_k x_k}^t \mathbf{K}^*$, where

$$\mathbf{B}_{x_k x_k}^t = \mathbf{B}_{x_k x_k}^{t-1} + \hat{\mathbf{Z}}_t^k \hat{\mathbf{Z}}_t^{kT} - \check{\mathbf{Z}}_t^k \check{\mathbf{Z}}_t^{kT}, \quad (26)$$

with the *compact* updating and downdating data matrices

$$\hat{\mathbf{Z}}_t^k = \mathbf{K}^* \hat{\mathbf{Y}}_t^k \mathbf{V} \quad \text{and} \quad \check{\mathbf{Z}}_t^k = \mathbf{K}^* \check{\mathbf{Y}}_t^k \mathbf{V}, \quad (27)$$

respectively, where \mathbf{K} is determined from (19) or (20), and

$$\mathbf{V} = \frac{1}{\sqrt{2}} \begin{bmatrix} \mathbf{I} & i\mathbf{I} \\ \mathbf{I} & -i\mathbf{I} \end{bmatrix}. \quad (28)$$

It should be noted that the transforms in (27) imply that \mathbf{Z}_t^k is real-valued. Here, we are interested in updating $(\hat{\mathbf{R}}_{x_k x_k}^t)^{-1}$. Such an update can be formed using the TVD structure of (26). A time-variant Toeplitz-like $M\bar{M} \times M\bar{M}$ matrix $\mathbf{B}_{x_k x_k}^t$ is said to have a TVD structure if the matrix difference $\nabla \mathbf{B}_{x_k x_k}^t$, defined by [6, 10]

$$\nabla \mathbf{B}_{x_k x_k}^t = \mathbf{B}_{x_k x_k}^t - \mathbf{F}_t \mathbf{B}_{x_k x_k}^{t-\Delta} \mathbf{F}_t^*, \quad (29)$$

has low *rank*, say $r(t)$, where $r(t) \ll M\bar{M}$, for some lower triangular matrix \mathbf{F}_t . The TVD rank, $r(t)$, provides a measure of the degree of structure present, with lower rank indicating stronger structure. Thus, if $r(t)$ is close to $M\bar{M}$, there is little point in pursuing the displacement framework. Combining (29) with (26) implies that

$$\nabla \mathbf{B}_{x_k x_k}^t = \hat{\mathbf{Z}}_t^k \hat{\mathbf{Z}}_t^{kT} - \check{\mathbf{Z}}_t^k \check{\mathbf{Z}}_t^{kT}, \quad (30)$$

where $\Delta = 1$, $\mathbf{F}_t = \mathbf{I}$, and the $M\bar{M} \times r(t)\bar{L}$ generator matrix $\hat{\mathbf{Z}}_t^k$ is used to update $\mathbf{B}_{x_k x_k}^t$ and matrix $\check{\mathbf{Z}}_t^k$ is used to downdate

⁴The time-updating using (26) requires only about half the number of operations compared to the update in (21).

$\mathbf{B}_{x_k x_k}^t$, respectively. Further, it can be seen that $r(t) = 2\bar{L}$ for both the updating and downdating generator matrices. We note that the positive-definite nature of $\mathbf{B}_{x_k x_k}^t$ guarantees the existence of a unique lower triangular Cholesky factor, \mathbf{C}_t , such that $\mathbf{B}_{x_k x_k}^t = \mathbf{C}_t \mathbf{C}_t^T$, which, exploiting (30), can be expressed in two stages as [10]

$$\begin{bmatrix} \hat{\mathbf{C}}_t & \mathbf{0} \end{bmatrix} \begin{bmatrix} \hat{\mathbf{C}}_t^T \\ \mathbf{0} \end{bmatrix} = \begin{bmatrix} \mathbf{C}_{t-1} & \hat{\mathbf{Z}}_t \end{bmatrix} \mathbf{I}_{n+m} \begin{bmatrix} \mathbf{C}_{t-1}^T \\ \hat{\mathbf{Z}}_t^T \end{bmatrix}$$

where $\hat{\mathbf{C}}_t$ represents the updated *only* Cholesky factor which is then followed by the downdating process below

$$\begin{bmatrix} \mathbf{C}_t & \mathbf{0} \end{bmatrix} \begin{bmatrix} \mathbf{C}_t^T \\ \mathbf{0} \end{bmatrix} = \begin{bmatrix} \hat{\mathbf{C}}_t & \check{\mathbf{Z}}_t \end{bmatrix} \begin{bmatrix} \mathbf{I}_n & \mathbf{0} \\ \mathbf{0} & \mathbf{I}_m \end{bmatrix} \begin{bmatrix} \hat{\mathbf{C}}_t^T \\ \check{\mathbf{Z}}_t^T \end{bmatrix}$$

in order to achieve both the up- and downdating (i.e., to effect the *sliding window*) of the Cholesky factors of the compact form of the FBA covariance estimate, $\mathbf{B}_{x_k x_k}^t$. Hence, it follows that there exists *two* $[\mathbf{I}_n \oplus \mathbf{I}_m]$ -unitary rotation matrices⁵, $\hat{\mathbf{\Gamma}}_t$ and $\check{\mathbf{\Gamma}}_t$, such that [10]

$$\begin{bmatrix} \hat{\mathbf{C}}_t & \mathbf{0} \end{bmatrix} = \begin{bmatrix} \mathbf{C}_{t-1} & \hat{\mathbf{Z}}_t \end{bmatrix} \hat{\mathbf{\Gamma}}_t, \quad (31)$$

and subsequently

$$\begin{bmatrix} \mathbf{C}_t & \mathbf{0} \end{bmatrix} = \begin{bmatrix} \hat{\mathbf{C}}_t & \check{\mathbf{Z}}_t \end{bmatrix} \check{\mathbf{\Gamma}}_t. \quad (32)$$

Note that $\hat{\mathbf{\Gamma}}_t$ and $\check{\mathbf{\Gamma}}_t$ have the effect of rotating the updating generator matrices, $\hat{\mathbf{Z}}_t$ and $\check{\mathbf{Z}}_t$, onto the expressions \mathbf{C}_{t-1} and $\hat{\mathbf{C}}_t$, respectively, to produce the up- and down dated Cholesky factor \mathbf{C}_t and block zero entries in the left-hand sides of (31) and (32). The rotation matrices $\hat{\mathbf{\Gamma}}_t$ and $\check{\mathbf{\Gamma}}_t$ can be formed in numerous different ways. Generally, however, Givens rotations are used for updating and Householder rotations for down-dating. As shown in [10], this procedure can easily be extended to also yield the inverse Cholesky factor; this is achieved by augmenting (31) with the inverse Cholesky factors according to [10]. By applying $\hat{\mathbf{\Gamma}}_t$ and $\check{\mathbf{\Gamma}}_t$, we thus find an efficient time-updating (sliding window) of the inverse Cholesky factor also, yielding one column vector per iteration. Using the updated inverse Cholesky factor, we form the time-updated covariance matrix estimate, using $\mathbf{L}_{x_k} = \mathbf{K}\mathbf{C}_{t-1}^{-1}$, in (13) and (16), where \mathbf{C}_t^{-1} represent the Cholesky factor of $(\hat{\mathbf{R}}_{x_k x_k}^t)^{-1}$. Combined with the time-updating of $\hat{\mathbf{R}}_{x_k x_k}$, evaluated reminiscent to (21), this forms the proposed time-updating algorithm. We finally remark that one may easily simplify the above time-updating to a exponential fading data-updating only scheme by omitting the downdate rotation and incorporating a forgetting factor.

⁵Here, a \mathbf{J} -unitary matrix Θ is defined as any matrix Θ such that $\Theta \mathbf{J} \Theta^* = \mathbf{J}$. Further, $\mathbf{a} \oplus \mathbf{b}$ denotes a matrix with the sub-matrices \mathbf{a} $\{n \times n\}$ and \mathbf{b} $\{m \times m\}$ concatenated to produce a matrix of size $\{(m+n) \times (m+n)\}$.

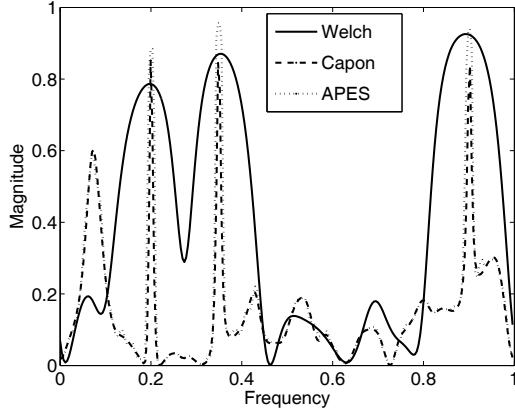


Fig. 1. MSC estimates for a 1-D data sequence.

4. NUMERICAL SIMULATIONS

For simplicity, we will initially assume two 1-D signals $x_1(n)$ and $x_2(n)$ that are only sharing three sinusoidal components, such that, $x_p(n) = \sum_{k=1}^3 \alpha_k^{(p)} e^{2\pi i f_k^{(p)} n} + w_p(n)$, where $\alpha_k^{(p)}$ and $f_k^{(p)}$ denote the (complex) amplitude and frequency of the k th sinusoid, of the p th signal, respectively. Here, $\alpha_k^{(1)} = 1$, $\forall k$, $f_1^{(1)} = 0.2$, $f_2^{(1)} = 0.35$ and $f_3^{(1)} = 0.9$. Further, $\alpha_k^{(2)} = \alpha_k^{(1)} e^{2\pi i \vartheta_k}$, where ϑ_k is a uniformly distributed random variable, between 0 and 2π . Finally, $w_1(n)$ and $w_2(n)$ are two independent zero-mean circularly symmetric Gaussian random processes with unit variance. For this example, the theoretical MSC should be unity at the frequencies f_k , $k = 1, 2, 3$, and zero elsewhere. Figure 1 shows the MSC estimates for the presented algorithms, as compared to the standard Welch's averaged periodogram technique, using $N = 64$ and $M = 16$. As is clear from the figure, both the Capon- and APES-based MSC estimators offer estimates significantly closer the true values. As expected [11], the APES-based estimator seems to offer a somewhat better amplitude estimates, although at the cost of a slightly wider peak, as compared to the Capon-based estimator. In the interest of brevity, we merely note that the above comparisons to the Welch-, Capon- and APES-based estimators will also hold for 2-D data sets. Figure 2 illustrates a 2-D MSC estimate of sinusoidal data. For an extended treatment of the 2-D results including error propagation performance, please see [12]. Finally, we examine the proposed time-updating of the MSC estimators. The cost of directly evaluating \mathbf{L}_{x_k} is about $\mathcal{O}(M^3 \bar{M}^3 + L \bar{L} M^2 \bar{M}^2)$ operations, including the cost of evaluating (17). As a comparison, using the proposed time-updating, \mathbf{L}_{x_k} can be found in about $\mathcal{O}(LM^2 \bar{M}^2)$ operations, omitting the need to update $\mathbf{R}_{x_k x_k}$ directly. For larger images, it is clear that the proposed updating offers a substantial complexity reduction as compared to the direct evaluation.

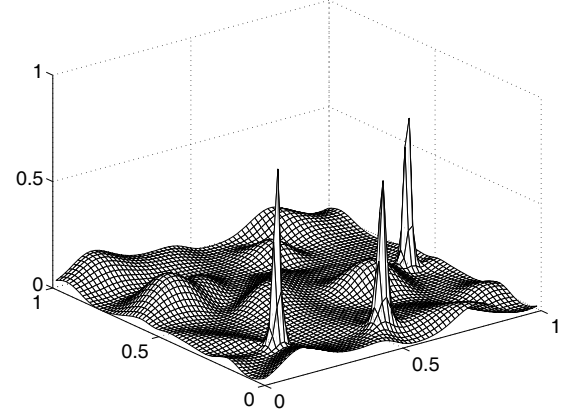


Fig. 2. The Capon-based 2-D MSC estimate.

5. REFERENCES

- [1] J. Li and P. Stoica, "Adaptive Filtering Approach to Spectral Estimation and SAR Imaging," *IEEE Trans. Signal Processing*, vol. 44, no. 6, pp. 1469–1484, June 1996.
- [2] P. Stoica and R. Moses, *Spectral Analysis of Signals*. Upper Saddle River, N.J.: Prentice Hall, 2005.
- [3] A. M. Guarnieri and C. Prati, "SAR Interferometry: A Quick and Dirty Coherence Estimator for Data Browsing," *IEEE Trans. on Geoscience and remote sensing*, vol. 35, no. 3, pp. 660–669, 1997.
- [4] R. Touzi, A. Lopes, J. Bruniquel, and P. W. Vachon, "Coherence Estimation for SAR Imagery," *IEEE Trans. Geosci. & Remote Sensing*, vol. 37, no. 1, pp. 135–149, January 1999.
- [5] J. Benesty, J. Chen, and Y. Huang, "A Generalized MVDR Spectrum," *IEEE Signal Processing Letters*, vol. 12, no. 12, pp. 827–830, December 2005.
- [6] T. Kailath and A. H. Sayed, *Fast Reliable Algorithms for Matrices with Structure*. Philadelphia, USA: SIAM, 1999.
- [7] A. Jakobsson, S. L. Marple, Jr., and P. Stoica, "Two-Dimensional Capon Spectrum Analysis," *IEEE Trans. on Signal Processing*, vol. 48, no. 9, pp. 2651–2661, September 2000.
- [8] E. G. Larsson and P. Stoica, "Fast Implementation of Two-Dimensional APES and Capon Spectral Estimators," *Multidimensional Systems and Signal Processing*, vol. 13, no. 1, pp. 35–54, Jan. 2002.
- [9] D. A. Linebarger, R. D. DeGroat, and E. M. Dowling, "Efficient Direction-Finding Methods Employing Forward/Backward Averaging," *IEEE Trans. Signal Processing*, vol. 42, pp. 2136–2145, August 1994.
- [10] A. H. Sayed, H. Lev-Ari, and T. Kailath, "Time-variant Displacement Structure and Triangular Arrays," *IEEE Trans. Signal Processing*, vol. 42, pp. 1052–1062, May 1994.
- [11] A. Jakobsson and P. Stoica, "Combining Capon and APES for Estimation of both Amplitude and Frequency of Spectral Lines," *Circuits, Systems, and Signal Processing*, vol. 19, no. 2, pp. 159–169, 2000.
- [12] A. Jakobsson, S. R. Alty, and J. Benesty, "Estimating and Time-Updating the 2-D Coherence Spectrum," *IEEE Transactions on Signal Processing*, to appear.